International Journal of Environment and Geoinformatics 11(2):001-009 (2024)

Research Article

Local Climate Zone Classification Using YOLOV8 Modeling in Instance Segmentation Method

Melike Nicanci Sinanoglu[1*], Sinasi Kaya[2]

[1] Department of Communication Systems, Graduate Education Institute, Istanbul Technical University, Istanbul, Turkey
[2] Department of Geomatics Engineering, Civil Engineering Faculty, Istanbul Technical University, Istanbul, Turkey

* Corresponding author: M. N. Sinanoğlu
E-mail: nicanci21@itu.edu.tr

Received 21.03.2024
Accepted 19.05.2024

How to cite: Nicanci Sinanoglu and Kaya (2024). Local Climate Zone Classification Using YOLOV8 Modeling in Instance Segmentation Method. *International Journal of Environment and Geoinformatics (IJEGEO)*, 11(2): 001-009. doi.10.30897/ijegeo.1456352

Abstract

Local climate zones play an important role in understanding microclimates in urban areas, contributing to urban planning, environmental sustainability and human comfort. Istanbul, a city connecting the European and Asian continents, creates microclimate diversity in city areas with the influence of different land use models. The concept of Urban Head Island (UHI) arises when urban areas have different temperatures with neighboring rural areas. The lack of a universally accepted definition of the concept of urban and rural areas has created difficulties in the evaluation of this concept. In response to this situation, a standardized Local Climate Zone (LCZ) classification system for urban temperature observations was created. This study performs LCZ classification with YOLOV8, one of the deep learning-based image segmentation models, using high-resolution Istanbul Google Earth images. Labeled data was created from WUDAPT's Google Earth images according to the post "Things to consider when creating LCZ training areas". Model training was carried out by creating a dataset by labeling high-resolution, bird's-eye view images of Istanbul obtained from Google Earth, paying attention to the diversity of LCZ categories. Box P 0.263, R 0.341, mAP50 0.317, mAP50-95 0.219 and Mask P 0.254, R 0.318, mAP50 0.404, mAP50-95 0.305 model metric values obtained after training were calculated. Although these values are below 50 percent, the LCZ class predictions appear to be largely accurate in the labeled result images. Metric results are important for improving the model and detecting weak points. This research contributes to the field of urban climate studies by providing a robust and scalable approach to LCZ classification using advanced deep learning techniques. The results can form the basis for urban planning, environmental sustainability and informed decision-making processes in the context of Istanbul's urban environment.

Keywords: local climate zones, deep learning, LCZ classification, instance segmentation, YOLOv8

Introduction

The city plays a crucial role in the ongoing development of human society. Urbanization stands out as one of the most significant phenomena globally today (Li, et al., 2019; Shen, et al., 2020; Wu, et al., 2020; Zhou, et al., 2020). As urbanization progresses, cities undergo substantial expansion, often at the expense of encroaching upon agricultural land and green open spaces (Zhou, et al., 2020; Huang and Wang, 2020; Shao, et al., 2020). Simultaneously, there is a significant influx of population into urban areas, contributing to urban growth (Li, et al., 2016; Trinder and Liu, 2020; Shao, et al., 2021).

Increasing urban populations and simultaneous ecological threats pose formidable challenges for cities grappling with the repercussions of rapid urbanization (Alsaaideh, et al., 2017). The 20th century witnessed a rapid increase. This rapid increase has led to the transformation of natural landscapes in urban areas into artificial surfaces, buildings and roads, causing significant changes in the urban area and climate (Taha, 1997). Cities, urban expansion, as we overcome the complexity of population growth and ecological problems, there is a need to balance solutions with environmental sustainability. The Urban Heat Island (UHI) effect, which is defined as the increase in temperature within a city differently than the temperature of neighboring rural areas (Memon, et al., 2008), is worsened by rapid urbanization and changes in land cover (Ruiz and Correa, 2015). The Urban Heat Island (UHI) effect stands out as an important environmental problem resulting from irregular and unplanned city construction during the urbanization process (Yang, et al., 2020). UHI manifests itself as higher temperatures in urban areas compared to neighboring rural areas. Researchers revealed the UHI intensity with traditional measurements by examining the temperature difference in urban and rural areas (Jiang, et al., 2006; Zheng, et al., 2018; Steward and Oke, 2012; Hadeel, et al., 2009; Zhou, et al., 2020; Huang, et al., 2021). The UHI effect occurs for many reasons. In addition to factors that people can control such as green areas, building materials, building heights, parking areas, and building spacing, natural factors such as wind speed, cloudiness, aspect, elevation, and water areas also affect this situation. Both sets of factors are important in influencing the formation of urban heat islands. The main sources of heating in cities include human-induced heat sources such as traffic, power plants, home heating and cooling systems, as well as factors that people can control. In addition, the absorption and dissipation of heat by complex urban structures also causes warming in cities (Memon, et al., 2008; Diren

Ustün, et al., 2022). Research has shown that urban green spaces provide cooling and increase outdoor thermal comfort during hot seasons. These green spaces can significantly reduce environmental stress caused by heat island effects (Akpinar, 2016).

Considering the constraints of the built urban landscape, which is especially evident in vibrant metropolises such as Istanbul, the necessity of increasing green areas becomes very important. In order to expand green areas, roofs, facades and roadsides should be determined as priority areas, and special attention should be paid to areas that lack green areas and are faced with high population density and building density (Kuscu Simsek and Sengezer, 2012). One of the problems experienced in densely populated areas is temperature fluctuation. One of the problems experienced in densely populated areas is temperature fluctuation. Considering these, it is necessary to prevent the problems arising from unplanned cities built without considering the future, especially in developed and constantly developing cities that receive constant migration, such as Istanbul.

The lack of universal definitions for determining urban and rural areas makes it difficult to classify these areas. This uncertainty in the classification of urban and rural areas makes it significantly difficult to accurately assess the Urban Heat Island (UHI) effect. The scope and rigor of UHI research may be limited due to the lack of a standardized classification. The Local Climate Zone (LCZ) scheme has emerged as an important classification system that provides a standardized framework for urban temperature observations in studies of the UHI impact. The LCZ classification system not only facilitates UHI research but also sets a standard for understanding urban temperature dynamics worldwide. The increasing adoption of deep learning algorithms for LCZ classification further increases the potential of LCZ classification. Before the advent of Local Climate Zone (LCZ) algorithms, the difference between urban areas and neighboring rural areas was examined to measure Urban Heat Island Intensity (UHII), a commonly used indicator to characterize the UHI impact. (Estoque, R.C.,2016). However, as urbanization progressed and urban-rural boundaries blurred, the method of comparing rural and urban hindered accurate UHI characterization.

Stewart and Oke (2012) introduced the LCZ scheme to objectively classify urban and rural land covers by considering the developmental impact on local temperatures. They suggested using LCZ X – LCZ D to represent KSE; where the KSE temperature is defined as the temperature of any LCZ (LCZ X) minus the temperature of LCZ D (Estoque., 2016). LCZ classes are shown in “Fig.1”. Recent years have seen a surge in global LCZ studies, particularly dominated by research in China (Yang, et al., 2019) and the United States (Middel, et al., 2014). Various countries and regions have undertaken empirical research combined with LCZ, expanding its applications beyond its initial intent for field site classification in UHI studies (Stewart, et al., 2014). In its first decade, LCZ applications have diversified, with a review of the range of represented research topics using biometric tools. This comprehensive overview identifies future trends for LCZ applications in urban research.

Mapping studies using the LCZ classification system are carried out with different techniques. Although classification with deep learning techniques is one of these techniques, the newest image segmentation models have not been used in LCZ classification and have not been used to detect LCZ changes more clearly and quickly in metropolitan city areas such as Istanbul, where LCZ classes can change. This paper working on these issues in this article, we aim to make the detection of LCZ changes in city areas more clearly and quickly with the new segmentation model developed. In the following sections, the article is explained as working area dataset preparation for image segmentation, creating a labeled dataset for the segmentation model, the method and model used for segmentation, model results, and finally the summary and conclusion of the study.

Study Area and Dataset

Our study focuses on the dynamic and culturally rich city of Istanbul, a unique metropolis spanning two continents, Europe and Asia, as seen in “Fig.2”. Istanbul, with its strategic location at the crossroads of diverse cultures, presents a compelling urban environment for the exploration of Local Climate Zones (LCZs). The geographical scope of our investigation includes key districts and neighborhoods within the expansive metropolitan area of Istanbul, covering approximately 5,343 km². Istanbul's distinctive geographic features include the Strait of Istanbul (Bosporus), which separates the European and Asian sides of the city, contributing to its climatic diversity. Istanbul experiences a Mediterranean climate, characterized by hot, dry summers and mild, wet winters. The city's topography, historic architecture, and modern developments create a mosaic of LCZs, as seen in “Fig.1” ranging from compact low-rise (LCZ 3) areas with preserved historical structures, such as the iconic Hagia Sophia and Blue Mosque, to zones with intensive industrial activities (LCZ 8 and LCZ 10) reflecting the city's economic vibrancy. Midrise and high-rise compact buildings from the build cover LCZ classes seen in “Fig.1” are very common in Istanbul.

Istanbul's urban fabric is a mixture of residential, commercial and industrial land uses and has a diverse urban landscape. It aims to use the Local Climate Zone (LCZ) classification to better understand Istanbul's microclimates and temperature changes in urban areas. The main factors affecting Istanbul's LCZs can be listed as urban development, historical preservation efforts and the challenges created by population growth. The city's water resources, including the Sea of Marmara, the Golden Horn and lakes, add another dimension to the climate dynamics (LCZ G). This study, an analysis of Istanbul's LCZs, aims to add valuable information that can be used as a basis for urban planning, climate impact analysis and sustainable environmental practices tailored to the specific needs of this dynamic and developing metropolis.

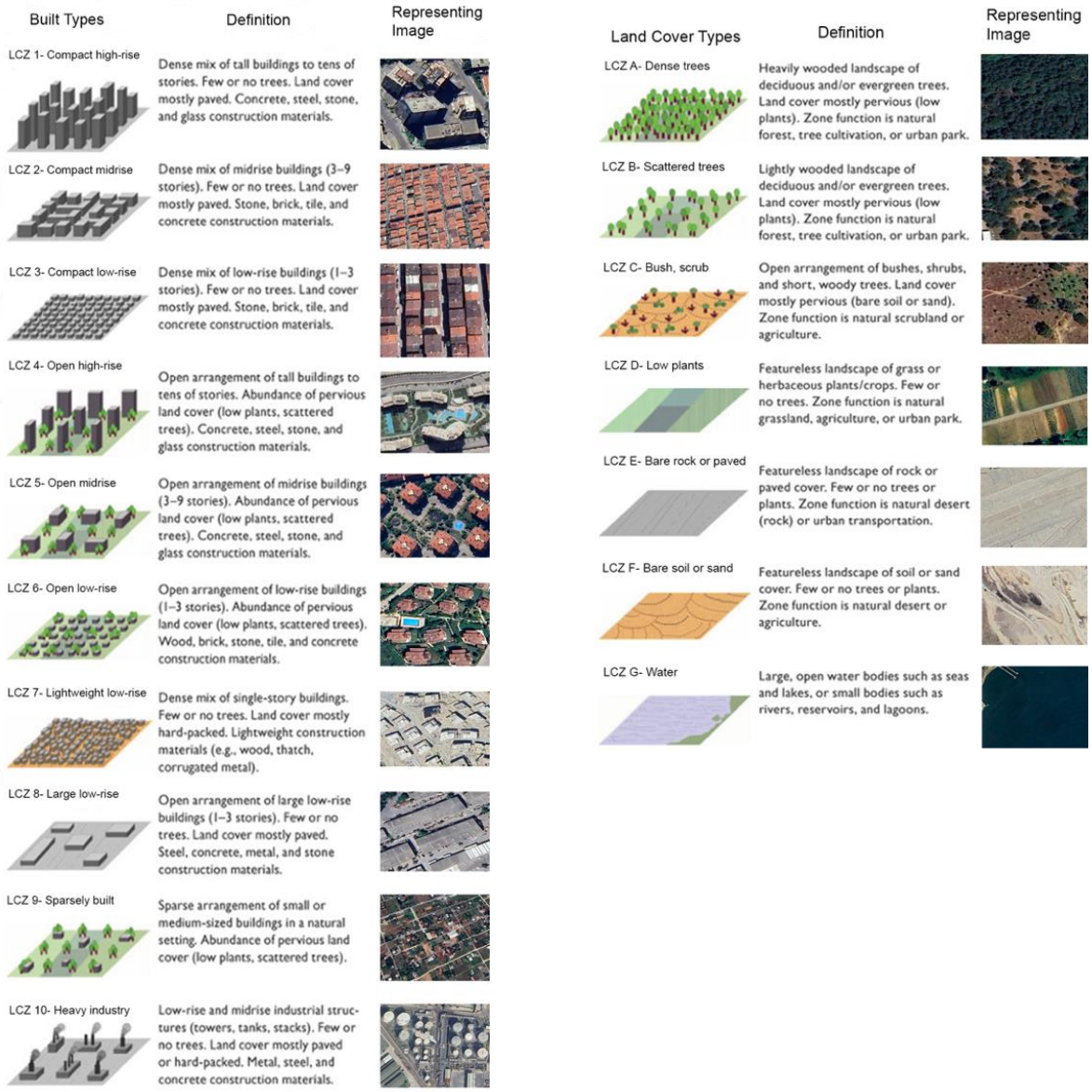

Fig 1. Local climate zones with illustration and representation image. (Steward and Oke, 2012)

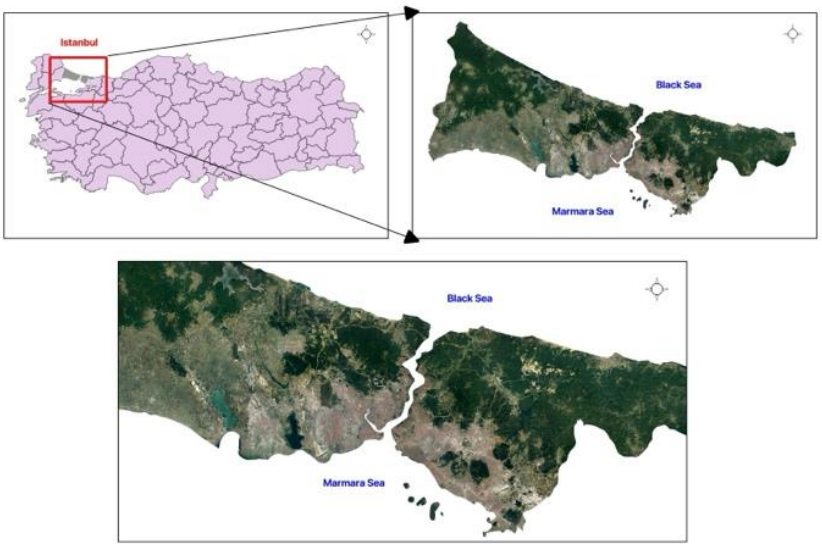

Fig. 2. Location of Istanbul (a); Google Earth satellite image of Istanbul (b).

Dataset and Pre-Processing

While creating the dataset for Local Climate Zone (LCZ) classification, Google Earth's high-resolution instant access and up-to-date satellite images, which are available as an open source to obtain geospatial information, were used. Combining satellite imagery, aerial photographs, and interactive maps, Google Earth provides researchers with a versatile resource for data collection and analysis.

Google Earth makes it easy to explore geographic features, land cover, and urban morphology with high-resolution satellite imagery. This platform is the ideal tool to define Local Climate Zones (LCZs) based on visual analysis, allowing researchers to virtually navigate between study zones. Figure 3 shows Istanbul city images taken from Google Earth for LCZ classification. As can be seen from the examples here, being able to designate the work area for research, quick access, high quality images and high quality downloadability are features that make study easier.

The decision to utilize Google Earth data in LCZ classification arises from several advantages:

- Global Coverage: Enables studying diverse urban environments worldwide.
- High-Resolution Imagery: Provides detailed urban landscape analysis.
- Temporal Analysis: Facilitates tracking urban development over time.
- Cost-Effectiveness: Economical compared to traditional methods.

While Google Earth offers significant advantages, researchers must be mindful of certain limitations. The temporal resolution may not be as frequent as dedicated satellite missions, and cloud cover can obscure visibility in some regions. Additionally, the use of Google Earth is subject to its terms of service and licensing agreements.

In conclusion, Google Earth emerges as a valuable resource for researchers engaged in the creation of LCZ classification datasets. Its global coverage, high-resolution imagery, temporal analysis capabilities, and cost-effectiveness contribute to the efficiency and accessibility of LCZ studies, fostering advancements in urban climate research.

Fig. 3. Google Earth images from some parts of Istanbul

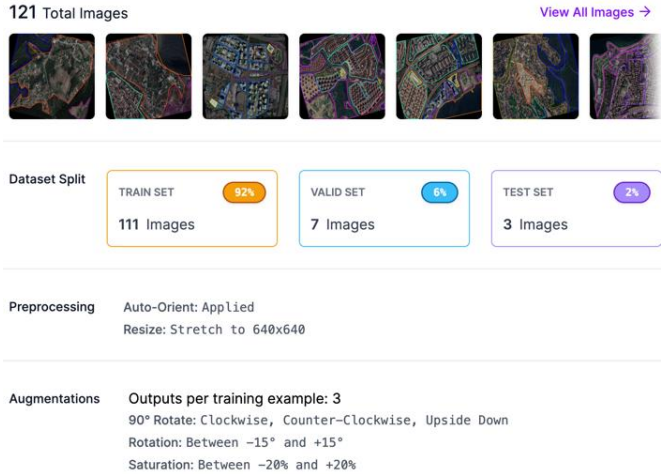

Fig.4. Total numbers of train, validation and test after data augmentation

Preparing Label Data

A dataset of 47 images was created for Local Climate Zone (LCZ) classification. Each image from Google Earth has a resolution of 1024x768 pixels. The dataset contains 17 different LCZ tags, with each image meticulously tagged. The labeled data then went through pre-processing and data augmentation processes. As seen in "Fig.4", the dataset with pre-processing and data augmentation resulted in a total of 121 labeled data.

Pre-processing steps such as auto-orient and resize are standards set for images. The standard image size in this study is 640x640 pixels. As seen in "Fig.4", three different data augmentation methods were used: clockwise, counterclockwise and upside down, rotating 90 degrees, rotating between ±15 degrees and changing saturation degrees between ±20 degrees. The reason for using these is that smaller points can be detected by preventing excessive learning during training.

Method

In the study, the YOLOv8 model, the newest and latest technology that can be used in object detection, image classification and sample segmentation tasks, was used. The YOLO (You Only Look Once) architecture has proven to be a robust and effective framework for object detection tasks. The working logic of the YOLO architecture is to evaluate input images by dividing them into grids. Evaluation is made according to whether an object exists in each grid formed and whether the midpoint of the object is found or not. YOLOv8, one of the versions of the YOLO architecture, offers improvements that make it particularly suitable for the Local Climate Zone (LCZ) classification. YOLOv8 uses a unified neural network for simultaneous bounding box prediction and class probabilities. Unlike traditional two-stage detectors, YOLOv8 processes images in a single pass, making it faster and more efficient; making it vital for large-scale datasets and real-time applications in LCZ classification. YOLOv8 includes many basic features in terms of visual classification performance. It uses a versatile backbone architecture that enables capturing complex classes and spatial relationships in urban environments. This feature is necessary for feature extraction from images. The YOLO layer in the architecture efficiently estimates object bounding boxes and class probabilities, making it suitable to use the model to detect various classes of LCZs encountered in urban environments. Multi-scale prediction capabilities allow objects of different sizes to be detected. This feature significantly increases the model's capacity to distinguish fine details in the LCZ classification, allowing accurate identification of urban structures and features without being affected by size differences of objects.

Advantages of YOLOv8 for LCZ Classification:

- Efficiency: YOLOv8's single-pass architecture enables fast image processing ideal for LCZ classification tasks and real-time applications.
- Adaptability: Flexible backbone architecture provides effective feature extraction, making it easier to detect various urban areas encountered in LCZ classification.
- Multi-Scale Capability: this capability increases the performance of recognizing various urban structures in fine detail without being affected by size differences, meeting the requirements of the LCZ classification.

As of January 10, 2023, there are five versions of YOLOv8, from YOLOv8n (the smallest model with a 37.3 mAP score on COCO) to YOLOv8x (the largest model with a 53.9 mAP score on COCO) (Ultralytics). COCO (Common Objects in Context) is the industry standard benchmark for evaluating object detection models. When comparing models on COCO, we look at the mAP value and FPS measurement for inference speed. Models should be compared at similar inference speeds. "Fig.5" shows the inference speed comparison of the Yolov8 model with other models. "Table 1" shows the accuracy of YOLOv8 model versions in COCO.

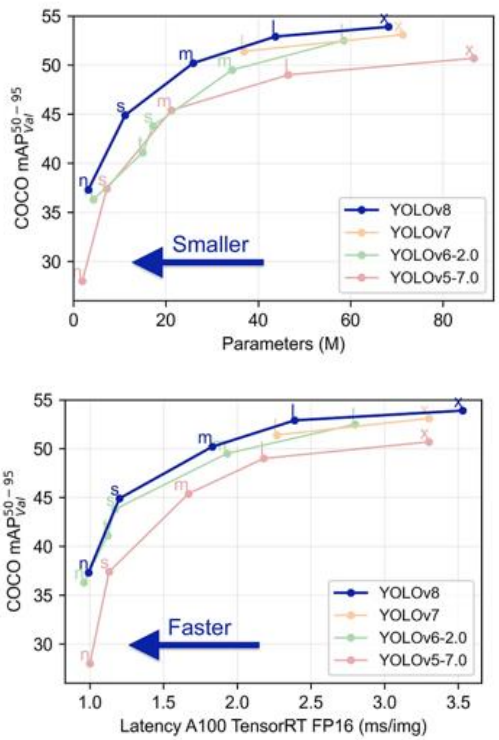

Fig. 5. A comparison between YOLOv8 and other YOLO models (Ultralytics)

In summary, YOLOv8's working principle, feature highlights, and advantages position it as a compelling choice for LCZ classification tasks, offering efficiency, adaptability, and multi-scale capabilities that are essential for accurately delineating the intricate features of urban environments.

There are some preliminary preparations required for model training with Yolo. Some of these preparations include labeling the images and creating a dataset, which we mentioned in the previous sections. When the created

dataset is ready for use, some parameters must be determined in order to optimize the performance of the model. The parameters and configurations employed during the training of Yolo models encompass a range of hyperparameters. These factors play a pivotal role in determining the model's effectiveness, velocity, and precision. Fundamental training configurations involve batch size, learning rate, momentum, and weight decay. Furthermore, the selection of optimizer, loss function, and composition of the training dataset can significantly influence the training procedure. Diligent fine-tuning and experimentation with these configurations are essential for maximizing performance.

Table 1. YOLOv8 COCO evaluation (Ultralytics)

Model	Size (pixels)	mAP val 50-95	Speed CPU ONNX (ms)	Speed A100 Tensor RT (ms)	params (M)	FLOPs (B)
YOLO v8n	640	37.3	80.4	0.99	3.2	8.7
YOLO v8s	640	44.9	128.4	1.20	11.2	28.6
YOLO v8m	640	50.2	234.7	1.83	25.9	78.9
YOLO v8l	640	52.9	375.2	2.39	43.7	165.2
YOLO v8x	640	53.9	479.1	3.53	68.2	257.8

Although some parameters come as Default, some are determined specifically according to the model. Specifically determined model parameters are shown in "Table 2". Epoch, signifies the complete passes made over the dataset during training. Adjusting this value impacts both the duration of training and the performance of the model. Epoch 150 was chosen here because at this point the performance of the model no longer changes significantly.

Table 2. Model hyperparameters

Epochs	Patience	Batch	Img. size
150	50	16	640

Patience helps prevent overfitting by stopping training when the model's performance reaches a plateau. Patience value is given as 100 by default, but 50 was chosen because the dataset is not large. Batch size for training determines the number of images processed before updating the model's internal parameters. 16 batches are sufficient for GPU memory usage. All images were selected at size 640 to eliminate computational complexity and increase model accuracy.

Results

As a result of modeling with Yolov8 architecture using the Istanbul Google Earth images dataset, the Local Climate Zone (LCZ) classification model was developed. The confusion matrix results of the dataset used for this modeling is shown in "Fig.6". The model was trained on 47 satellite images, and the results indicate high accuracy in classifying LCZ A and LCZ G. However, further training is needed, especially for distinguishing LCZ1-2-3 in urban areas where it appears challenging.

In particular, LCZ B and LCZ C exhibit some points of confusion in the classification. Additionally, distinguishing between LCZ E and LCZ 8 poses a challenge and shows overlaps with other confused classes. Upon reviewing the results, it is evident that additional visual support is required for the LCZ model training.

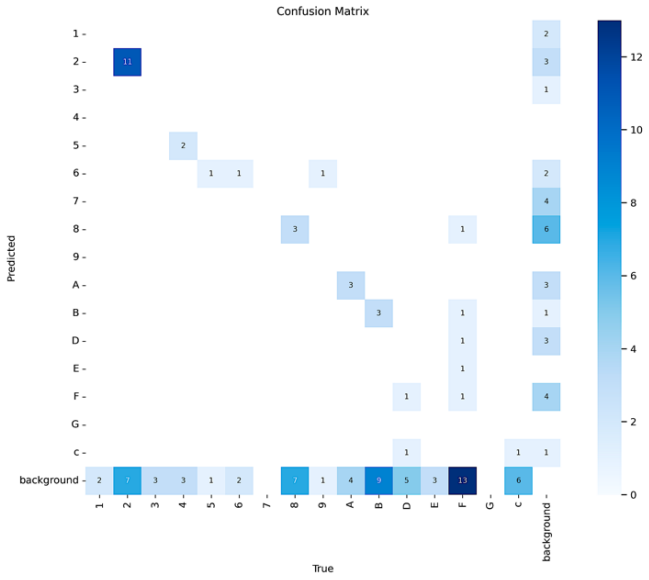

Fig. 6. Confusion matrix of model dataset

The current model may benefit from more focused training on LCZ1-2-3 differentiation in urban settings, as well as addressing the confusion points between LCZ B and LCZ C. Furthermore, efforts should be directed towards refining the model's ability to distinguish between LCZ E and LCZ 8.

Tablo 3. Model Metrics

	P	R	mAP50	mAP 50-95
Box	0.263	0.341	0.317	0.219
Mask	0.254	0.318	0.404	0.305

"Table 3" above contains the results of various metrics used to measure the performance of the model.

- Box (P, R, mAP50, mAP50-95): This indicates the precision (P), recall (R), and average precision (mAP) of bounding boxes for object detection. mAP50 represents the average precision calculated using the threshold value corresponding to 0.5. mAP50-95 represents the average precision calculated using threshold values between 0.5 and 0.95.
- Mask (P, R, mAP50, mAP50-95): This shows the precision (P), recall (R), and average precision (mAP) of masks for instance segmentation. Mask mAP50 represents the average precision calculated using the threshold value corresponding to 0.5. Mask mAP50-95 represents the average precision calculated using threshold values between 0.5 and 0.95.

When the metric results are evaluated, we see that the results do not exceed 50 percent. This is an expected result due to the small size of the data set used. Low values here do not mean that the segmentation is working incorrectly. Whether the values are acceptable or not can be evaluated as a result of comparisons with different datasets and models. These measurements are necessary results to help improve the model and understand weak points.

Summary and Conclusions

The results classified according to the model using Istanbul images are shown in "Fig.7". Expressions 1-9 and A-G in these images are abbreviations for LCZ classes, Structure Types LCZ 1-9 and Land Cover Types LCZ A-G. The decimal expressions indicated in the images are percentage results (0.3 percent to 30 percent) and represent an estimate of which LCZ class the marked region belongs to. In examining the result visuals in "Fig.7", it is evident that labeled images with low prediction probabilities often reveal accurate predictions upon closer inspection. Despite low predicted probabilities, the model demonstrates a consistent ability to make correct predictions. However, it underlines the need for a data set prepared with more detailed and qualitatively increased images in regions where LCZ classification is difficult to distinguish.

The analysis suggests that low classification predictions cannot be misclassification per se and that a different method and larger training data are required to gain a more detailed understanding of the model's performance. Examination of the visual classification of challenging LCZ classes shows that the model tends to provide accurate LCZ classifications although the predicted probabilities are low.

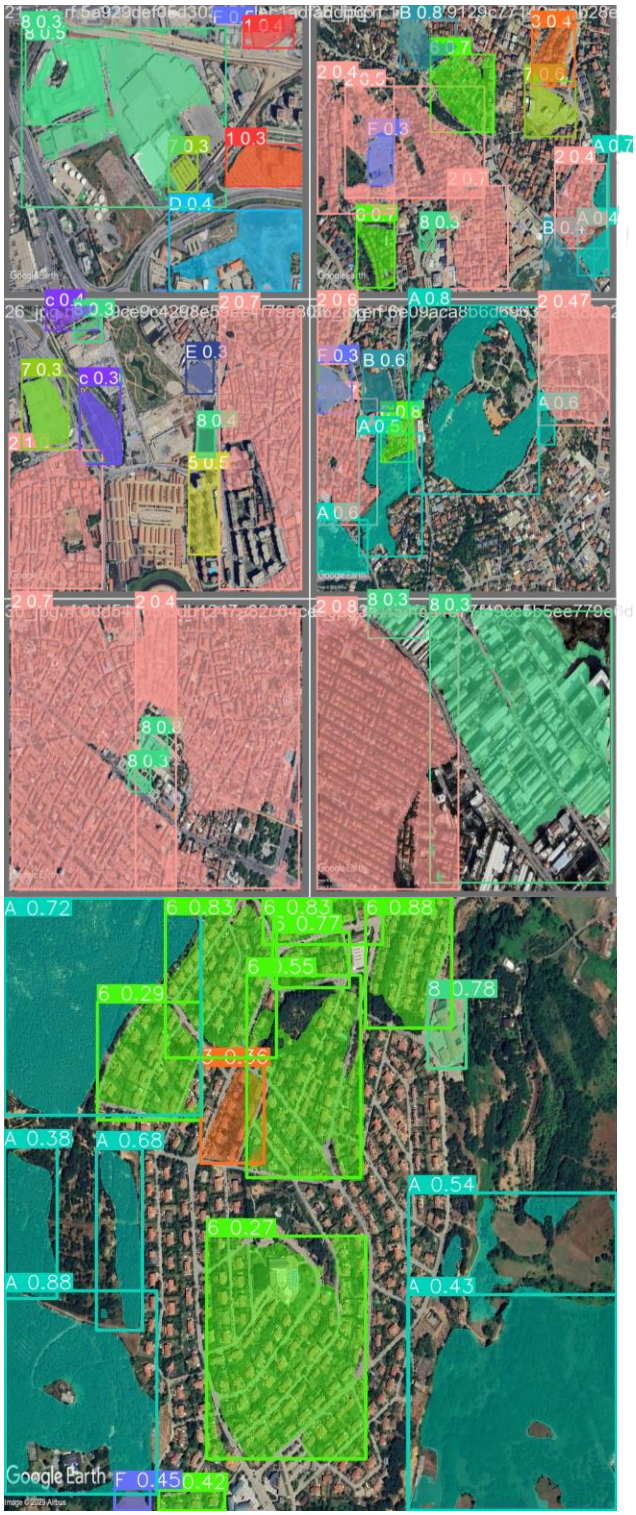

Fig. 7. Images labeled as a result of modeling

It is recommended to use a more carefully selected, larger data set to improve the performance of the model by

removing areas of confounding. Once these adjustments are made, a dataset that captures the complexity of LCZ features even in challenging scenarios can contribute to achieving high-accuracy LCZ classifications without the need for extensive manual review.

As a result, although the model provides effective results in general, there is a need to increase the quality of the data set and make improvements to the model, especially in areas prone to confusion. Knowing the region and creating a classification model in smaller areas can also contribute to improvement. While creating the data set, street images of the region as well as satellite images can be examined and visual interpretation can be strengthened to improve the model. The findings underscore the importance of dataset optimization in achieving reliable and accurate LCZ classification results. It is seen as a clear conclusion that a good modeling result can be achieved with a good data set and that LCZ classification can produce faster, more detailed and effective results even in difficult areas.

References

Akpinar, A. (2016). How is quality of urban green spaces associated with physical activity and health?. *Urban Forestry & Urban Greening*, 16, 76-83.

Alsaaideh, B., Tateishi, R., Phong, D.X., Hoan, N.T., Al-Hanbali, A., Xiulian, B. (2017). New Urban Map of Eurasia Using MODIS and Multi-source Geospatial Data. *Geo-spatial Information Science*, 20 (1), 29–38. doi:10.1080/10095020.2017.1288418.

Diren Ustun, D., Kaplan, E., Unal, Y. (2022). Istanbul Urban Heat Island and Its Change Due to Urban Development Scenarios. *Environment, Climate and Sustainability*, 23(1), 55–68.

Feng, W., Liu, J. (2022). A Literature Survey of Local Climate Zone Classification: Status, Application, and Prospect. *Buildings*, 12, 1693.

Hadeel, A., Jabbar, M., Chen, X. (2009). Application of Remote Sensing and GIS to the Study of Land Use/Cover Change and Urbanization Expansion in Basrah Province, Southern Iraq. *Geo-spatial Information Science*, 12 (2), 135–141. doi:10.1007/s11806-009-0244-7.

Huang, B., Wang, J. (2020). Big Spatial Data for Urban and Environmental Sustainability. *Geo-spatial Information Science*, 23 (2), 125–140. doi:10.1080/10095020.2020.1754138.

Huang, X., Liu, A., Li, J. (2021). Mapping and Analyzing the Local Climate Zones in China's 32 Major Cities Using Landsat Imagery Based on A Novel Convolutional Neural Network. *Geo-spatial Information Science*, 1–30. doi:10.1080/10095020. 2021.1892459.

Jiang, Z., Chen, Y., Jing, L. (2006). On Urban Heat Island of Beijing Based on Landsat TM Data. *Geo-spatial Information Science*, 9 (4), 293–297. doi:10. 1007/BF02826743.

Kuscu Simsek, C., Sengezer, S. (2012). The Importance of Green Areas in Reducing Urban Warming in the Istanbul Metropolitan Area. *Megaron*, 7(2): 116-128

Li, D., Ma, J., Cheng, T., van Genderen, J., Shao, Z. (2019). Challenges and Opportunities for the Development of Megacities. *International Journal of Digital Earth*, 12 (12), 1382–1395. doi:10.1080/17538947.2018.1512662.

Li, D., Zhao, X., Li, X. (2016). Remote Sensing of Human Beings – A Perspective from Nighttime Light. *Geo-spatial Information Science*, 19 (1), 69–79. doi:10.1080/10095020.2016.1159389.

Li, J., Song, C., Cao, L., Zhu, F., Meng, X., Wu, J. (2011). Impacts of landscape structure on surface urban heat islands: A case study of Shanghai, China. *Remote Sensing of Environment,* 115, 3249–3263.

Memon, R.A., Leung, D.Y., Chunho, L. (2008). A review on the generation, determination and mitigation of urban heat island. *Journal of Environmental Sciences*, 20, 120–128.

Middel, A., Häb, K., Brazel, A.J., Martin, C.A., Guhathakurta, S. (2014). Impact of urban form and design on mid-afternoon microclimate in Phoenix Local Climate Zones. *Landscape and Urban Planning*, 122, 16–28.

Ruiz, M.A., Correa, E.N. (2015). Adaptive model for outdoor thermal comfort assessment in an Oasis city of arid climate. *Building and Environment*, 85, 40–51.

Santamouris, M. (2014). Cooling the cities—A review of reflective and green roof mitigation technologies to fight heat island and improve comfort in urban environments. *Solar Energy*, 103, 682–703.

Shao, Z., Li, C., Li, D., Altan, O., Zhang, L., Ding, L. (2020). An Accurate Matching Method for Projecting Vector Data into Surveillance Video to Monitor and Protect Cultivated Land. *ISPRS International Journal of Geo-Information,* 9 (7), 448. doi:10.3390/ijgi9070448.

Shao, Z., Sumari, N.S., Portnov, A., Ujoh, F., Musakwa, W., Mandela, P.J. (2021). Urban Sprawl and Its Impact on Sustainable Urban Development: A Combination of Remote Sensing and Social Media Data. *Geo-spatial Information Science*, 24 (2), 241–255. doi:10.1080/10095020.2020.1787800.

Shen, P., Ouyang, L., Wang, C., Shi, Y., Su, Y. (2020). Cluster and Characteristic Analysis of Shanghai Metro Stations Based on Metro Card and Land-Use Data. *Geo-spatial Information Science*, 23 (4), 352–361. doi:10.1080/10095020.2020.1846463.

Stewart, I.D., Oke, T.R. (2012). Local Climate Zones for Urban Temperature Studies. *Bulletin of the American Meteorological Society*. 93. 1879-1900. 10.1175/BAMS-D-11-00019.1.

Stewart, I.D., Oke, T.R., Krayenhoff, E.S. (2014). Evaluation of the 'local climate zone' scheme using temperature observations and model simulations. *International Journal of Climatology*, 34, 1062–1080.

Taha, H. (1997). Urban climates and heat islands: Albedo, evapotranspiration, and anthropogenic heat. *Energy and Buildings*, 25, 99–103.

Trinder, J., Liu, Q. (2020). Assessing Environmental Impacts of Urban Growth Using Remote Sensing. *Geo-spatial Information Science*, 23 (1), 20–39. doi:10.1080/10095020.2019.1710438.

Wu, H., Gui, Z., Yang, Z. (2020). Geospatial Big Data for Urban Planning and Urban Management. *Geo-spatial*

Information Science, 23 (4), 273–274. doi:10.1080/10095020.2020.1854981.

Yang, C., Zhan, Q., Gao, S., Liu, H. (2020). Characterizing the Spatial and Temporal Variation of the Land Surface Temperature Hotspots in Wuhan from A Local Scale. *Geo-spatial Information Science*, 23 (4), 327–340. doi:10.1080/10095020. 2020.1834882.

Yang, J., Jin, S., Xiao, X., Jin, C., Xia, J.C., Li, X., Wang, S. (2019). Local climate zone ventilation and urban land surface temperatures: Towards a performance-based and wind-sensitive planning proposal in megacities. *Sustainable Cities and Society*, 47, 101487.

Zheng, Y., Ren, C., Xu, Y., Wang, R., Ho, J., Lau, K., Ng, E. (2018). GIS-Based Mapping of Local Climate Zone in the High-Density City of Hong Kong. *Urban Climate*, 24, 419–448. doi:10.1016/j.uclim. 2017.05.008.

Zhou, L., Shao, Z., Wang, S., Huang, X. (2022). Deep learning-based local climate zone classification using Sentinel-1 SAR and Sentinel-2 multispectral imagery. *Geo-spatial Information Science*. 25. 10.1080/10095020.2022.2030654.

Zhou, Q., Zhai, M., Yu, W. (2020). Exploring Point Zero: A Study of 20 Chinese Cities. *Geo-spatial Information Science* 23 (3), 258–272. doi:10.1080/10095020. 2020.1779011.

Zhou, X., Okaze, T., Ren, C., Cai, M., Ishida, Y., Mochida, A. (2020a). Mapping Local Climate Zones for a Japanese Large City by an Extended Workflow of WUDAPT Level 0 Method. *Urban Climate*, 33, 100660. doi:10.1016/j.uclim.2020.100660.

Zhou, X., Okaze, T., Ren, C., Cai, M., Ishida, Y., Watanabe, H., Mochida, A. (2020b). Evaluation of urban heat islands using local climate zones under the influences of sea-land breeze. *Sustainable Cities and Society*, 55, 102060. doi:10.1016/j.scs.2020.102060.